A probabilistic spatio-temporal model for vent opening clustering at Campi Flegrei caldera (Italy)

AGU fall meeting: Paper Number NH53B – 3887
Abstract ID: 22112

A. Bevilacqua (1,2), R. Isaia (3), F. Flandoli (4), A. Neri (1), D. Quaranta (4), S. Vitale (5)

(1) Istituto Nazionale di Geofisica e Vulcanologia, Sezione di Pisa, Pisa, Italy, (2) Scuola Normale Superiore di Pisa, Pisa, Italy, (3) Istituto Nazionale di Geofisica e Vulcanologia, Osservatorio Vesuviano, Napoli, Italy, (4) Università di Pisa, Dip.to di Matematica, Pisa, Italy, (5) Università di Napoli "Federico II", Dip.to di Scienze della Terra, dell'Ambiente e delle Risorse, Napoli, Italy

Introduction

Campi Flegrei (CF) is a densely urbanized caldera with a very high volcanic risk. Its more recent volcanic activity was characterized in the last 15 kyrs by more than 70 explosive events of variable scale and vent location. The sequence of eruptive events at CF is remarkably inhomogeneous, both in space and time. Activity has been subdivided into three distinct epochs, alternated by long periods of quiescence, and the stratigraphic record shows the presence of clusters of eruptions in space-time even inside the single epochs of activity.

In particular the opening of a vent in a particular location and at a specific time seems to increase the probability of another vent opening in the nearby area and in the next decades-centuries (self-exciting effect). Hence a time-space mathematical model has been developed, taking into account both the quantification of the significant uncertainty affecting the eruptive record and the possible self-exciting behaviour of the system.

Here are presented:

- a probabilistic model with uncertainty for past eruption data: time, location and volume of dense rock equivalent (VDRE) erupted;
- the plots of erupted volumes as a function of time, associated with the occurrence of local clusters of events and in general of a recurrent behaviour of the volcanic system;
- a doubly stochastic process aimed to represent the phenomenon of vent opening clustering, incorporating the effect of the sources of epistemic uncertainty on its parameters.

This kind of study is crucial to understand the possible time and scale of the next explosive activity, the likelihood and the consequences of Monte Nuovo (MN) in AD 1538 to be the first eruption of an incoming Epoch IV or not.

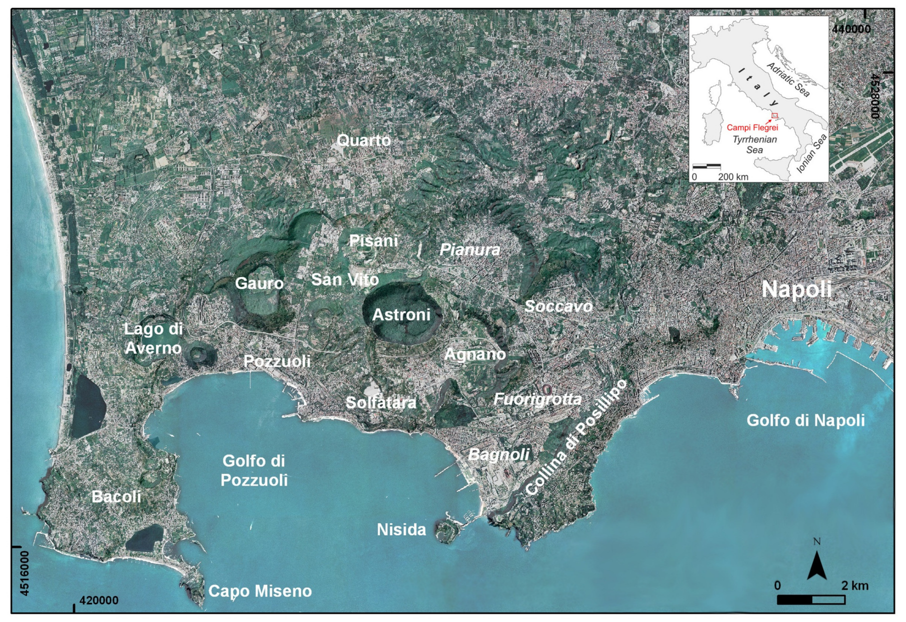

Fig 1. Mosaic of orthophotos of Campi Flegrei caldera and surrounding areas (including the city of Naples on the east) showing the large urbanization inside and around this active volcano. From Bevilacqua et al. [submitted].

The eruptive sequence dataset with uncertainty

The available geological record about past eruptive events includes four types of information:

- the ordered stratigraphic sequence of the eruptions (unsure in a few cases);
- some large dating time windows for a subfamily of the eruptions, i.e. 5th and 95th percentiles;
- VDRE estimates for the eruptions, some of them affected by a large uncertainty.

The stratigraphic dataset and the VDRE estimates largely rely on the work of Smith at al. [2011] with a few minor modifications and updates due to the most recent research findings and uncertainty assessments. The definition of the probability distribution of past eruptions time is produced by a Monte Carlo simulation, based on simple conditional sampling procedures (see also Bebbington and Cronin [2010]):

- the uncertain order of some of the events and the chance of simultaneous eruptions are randomly sampled;
- the time for the eruptions associated with dating time windows is then sampled, assuming symmetric triangular probability distributions with the given percentiles, and rejecting the samples that violate the stratigraphic order;
- the remaining subsequence of eruptions between the times just fixed, are sampled as ordered families of independent uniformly distributed random variables.

The spatial localization of past vents relies instead on the new data of Bevilacqua et al. [submitted]: the uniform ellipses of uncertainty (Fig 2) and the caldera partitioning (Fig 3) presented in that study are adopted. Each eruption has been associated with an element of the partition if its ellipse does not spread on more zones, or randomly sampled during the Monte Carlo simulation otherwise.

EPOCH III

ID	Name	Time min	Time max	VDRE (hm3) min		VDRE (hm3) max	E/W	Zone
28	Nisida	3213	4188	10	20	30	E	13
27	Fossa Lupara	3978	4192	10	20	30	E	7
26	Astroni 7	4098	4297	35	70	105	E	8
25	Astroni 6	-	-	60	120	180	E	8
24	Astroni 5	-	-	50	100	150	E	8
23	Astroni 4	-	-	70	140	210	E	8
22	Astroni 3	-	-	80	160	240	E	8
21	Astroni 2	-	-	10	20	30	E	8
20	Astroni 1	4153	4345	30	60	90	E	8
19	Averno 2	-	-	35	70	105	W	3
18	Solfatara	4181	4386	15	30	45	E	6
17	Accademia lava dome	-	-	0	-	10	E	6
16	Olibano tephra	-	-	10	-	100	E	6
15	Solfatara lava dome	-	-	0	-	10	E	6
14	Paleoastroni 3	-	-	10	20	30	E	8
13	Olibano lava dome	-	-	0	-	10	E	6
12	St. Maria delle Grazie	4382	4509	10	-	100	E	6
11	Agnano Monte Spina	4482	4625	425	850	1275	E	8 - 9
10	Paleoastroni 2	4712	4757	100	-	300	E	8
9	Paleoastroni 1	4745	4834	25	50	75	E	8
8	Monte Sant'Angelo	4832	5010	100	-	300	E	9
7	Capo Miseno	-	-	10	20	30	W	1
6	Pigniatiello 2	-	-	10	20	30	E	9
5	Cigliano	-	-	25	50	75	E	8
4	Agnano 3	-	-	95	190	285	E	9
3	Averno 1	5064	5431	10	-	100	W	3
2	Agnano 2	-	-	5	10	15	E	9
1	Agnano 1	5266	5628	10	20	30	E	9

EPOCH II

ID	Name	Time min	Time max	VDRE (hm3) min		VDRE (hm3) max	E/W	Zone
8	San Martino	9026	9370	25	50	75	E	7
7	Sartania 2	-	-	10	-	100	E	8
6	Pigna San Nicola	9201	9533	100	-	300	E	9
5	Costa San domenico	-	-	10	-	100	E	9
4	Monte Spina lava dome	-	-	0	-	10	E	9
3	Sartania 1	9500	9654	10	-	100	E	8
2	Fondi di Baia	9525	9695	20	40	60	W	2
1	Baia	-	-	0	-	10	W	2

EPOCH I

ID	Name	Time min	Time max	VDRE (hm3) min		VDRE (hm3) max	E/W	Zone
33	Porto Miseno	-	-	10	-	100	W	1
32	Bacoli	-	-	100	200	300	W	1
31	Casale	-	-	10	-	100	E	6 - 9 - 12
30	Pisani 3	10516	10755	10	-	100	E	7
29	Pignatiello 1	-	-	10	-	100	E	6 - 7 - 8 - 9 - 12
28	Montagna Spaccata	-	-	10	20	30	E	7
27	Concola	-	-	0	-	10	W	4
26	Fondo Riccio	-	-	0	-	10	W	4
25	Pisani 2	-	-	100	-	300	E	7
24	Pisani 1	-	-	100	-	300	E	7
23	Soccavo 5	-	-	10	-	100	E	11
22	Minopoli 2	-	-	10	-	100	E	11
21	Paleo San Martino	-	-	10	-	100	E	7
20	Soccavo 4	-	-	100	-	300	E	11
19	S4s3_2	-	-	10	-	100	E	8 - 9 - 10
18	S4s3_1	-	-	100	-	300	E	8 - 9 - 10
17	Soccavo 3	-	-	10	-	100	E	10
16	Soccavo 2	-	-	10	-	100	E	11
15	Paleo Pisani 2	-	-	100	-	300	E	7
14	Paleo Pisani 1	-	-	10	-	100	E	7
13	Pomici Principali	11915	12158	425	850	1275	E	8 - 9 - 10
12	Gaiola	-	-	10	-	100	E	13
11	Soccavo 1	-	-	250	500	750	E	11
10	Paradiso	-	-	10	-	100	E	11
9	Minopoli 1	-	-	10	-	100	E	11
8	Torre Cappella	-	-	10	-	100	W	2
7	La Pigna 2	-	-	10	-	100	E	11
6	La Pigna 1	12749	13110	10	-	100	E	11
5	La Pietra	-	-	10	-	100	E	6
4	Santa Teresa	-	-	10	-	100	E	12
3	Gauro	12721	15511	250	500	750	W	4
2	Mofete	-	-	10	-	100	W	2
1	Bellavista	-	-	10	-	100	W	2

Table 1. Record of times, erupted VDREs and locations (East-West and partition zone) of the events at Campi Flegrei, with uncertainty bounds. The VDRE estimates with values greater than or equal to 0.1 km³ are reported in red, the smaller than or equal to 0.01 km³ in blue.

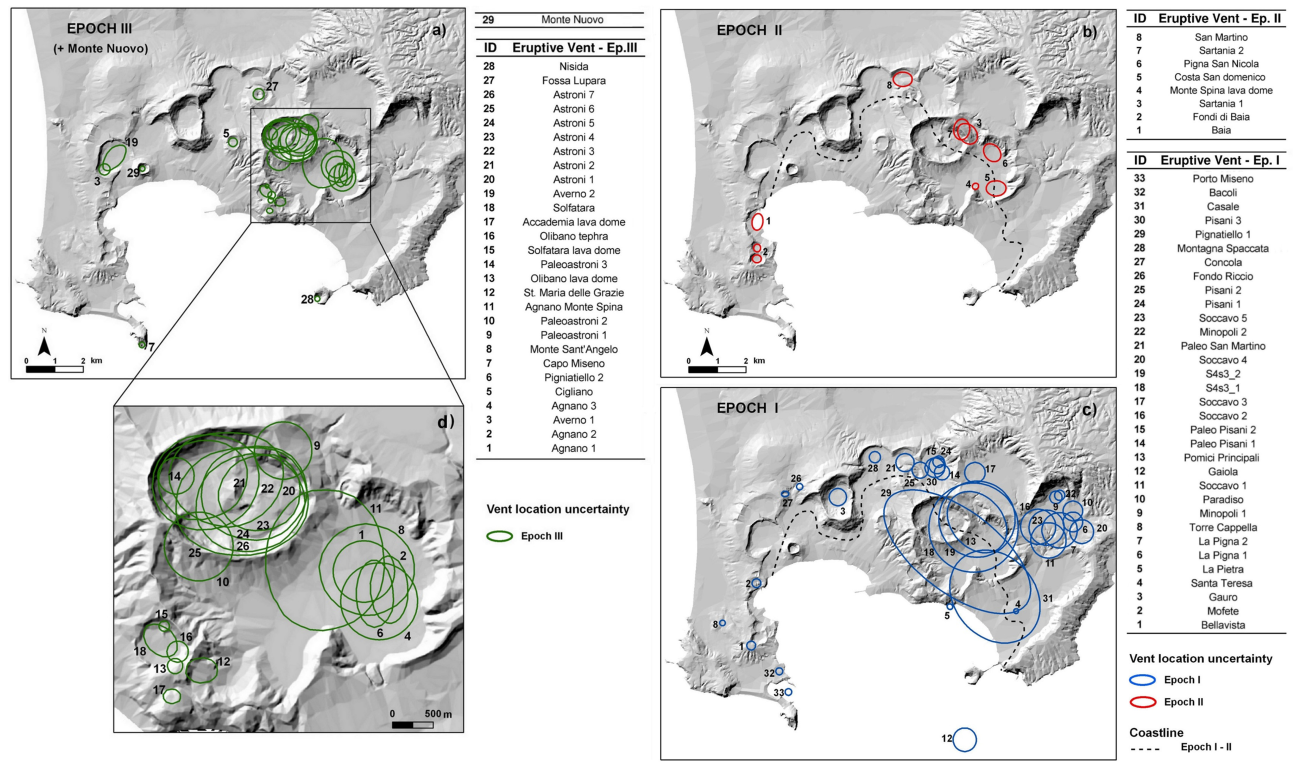

Fig 2. Reconstruction of the location of the eruptive vents and fissures for the events occurred in Epoch III (a), Epoch II (b), Epoch I (c). Numbered circles and ellipses indicate the assumed vent location of the events listed on the right side of the maps. The map shown in (d) represents an enlargement of the area of Agnano-Astroni-Solfatara where many events occurred. From Bevilacqua et al. [submitted].

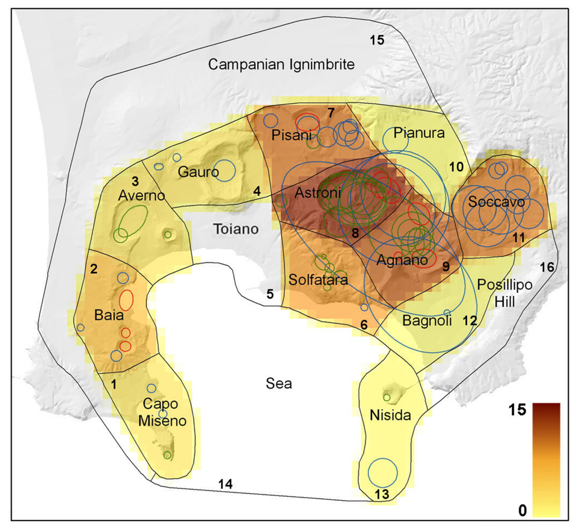

Fig 3. Partitioning of the caldera in 16 zones (Bevilacqua et al. [submitted]). The color represents the number of vents opened in each of the zones during all the three epochs.

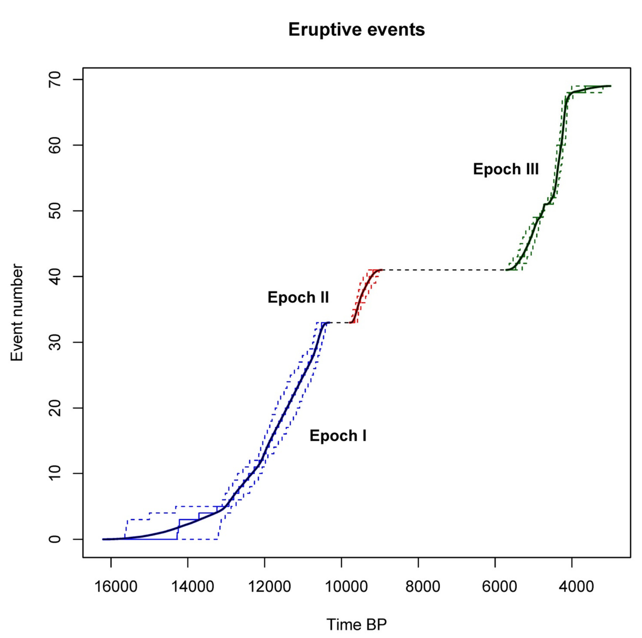

Fig 4. Cumulative event number as a function of time during the entire record considered assuming the probability model described above. The bold line is the mean value, the narrow line is the 50th percentile and the dashed lines are 5th and 95th percentiles of the uncertainty.

In Figure 4 is shown the eruptions number as a function of time and assuming the probability model for uncertainty described here. In particular looking at Epoch III it is evident a change of the eruption rate after the very large eruption of Agnano Monte Spina.

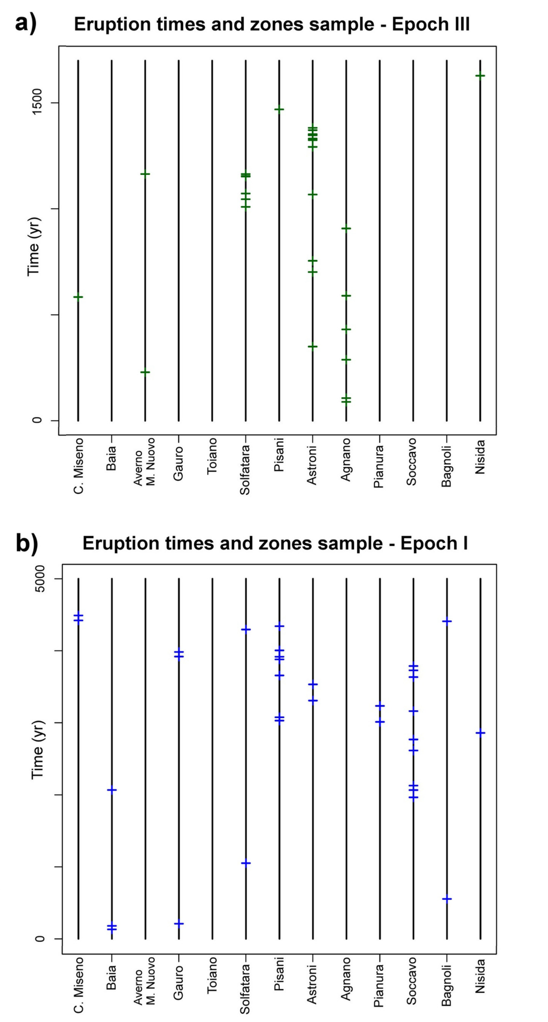

Fig 5. Random samples of eruption times and zones during Epoch III (a) and Epoch I (b). Each coloured line represents an event.

In Smith at al. [2011] some of the eruptions have a single valued VDRE estimate, other eruptions only inequality bounds. For the first is assumed a triangular sampling with 5th and 95th percentiles on ±50% relative errors, coherently with Klawonn et al. [2014]; the rest of the eruptions have been uniformly sampled inside three different intervals associated to different volume sizes: [0,0.01], [0.01,0.1], [0.1,0.3] Km³ (see Tab 1). It is planned a further research to refine and diversify these first estimates.

Figure 5 shows two samples of eruptions times and zones during Epoch I and III, the presence of clustering phenomena is quite evident.

Spatio-temporal description of erupted volumes

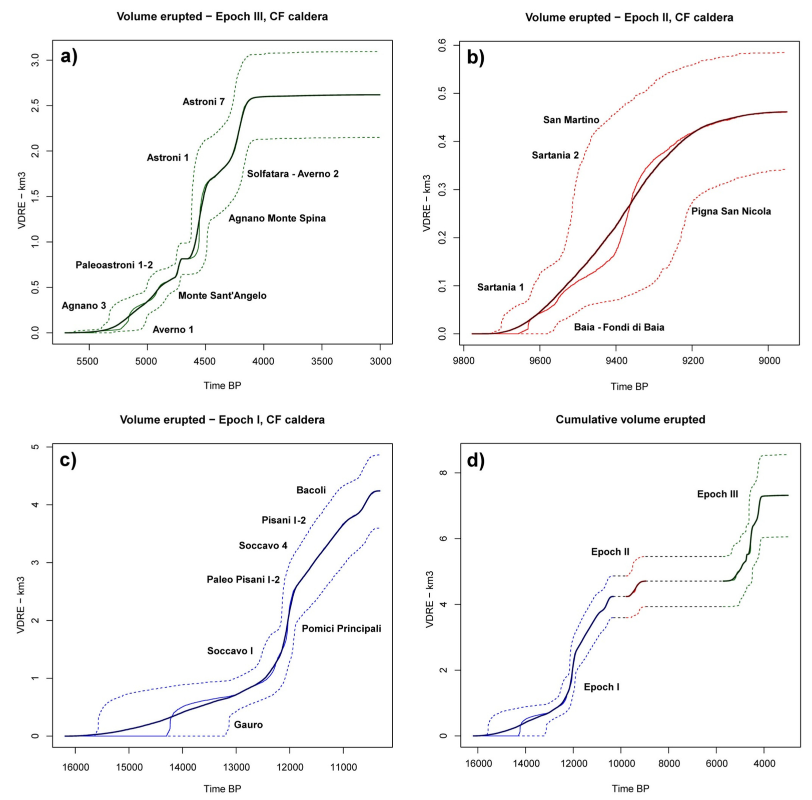

Fig 6. Cumulative volume erupted as a function of time during Epoch III (a), Epoch II (b), Epoch I (c) and then during the entire record considered (d), assuming the probability model described above. The bold line is the mean value, the narrow line is the 50th percentile and the dashed lines are 5th and 95th percentiles of the uncertainty.

From the eruptive record it is possible to observe the presence of clusters of events in space-time. In Figure 6 we show the cumulative erupted volumes: it is worth noting the different scale of Epoch II, involving volumes 5 times smaller than Epochs III and even 8 times smaller than Epoch I.

In Figure 7 the cumulative volumes erupted by the eastern part of the caldera are separated from the volumes from the western, that except for the significant activity of Gauro volcano in the Epoch I are remarkably smaller. It can be also noted that the activity in the West is associated to the initial and final phases of the eruptive epochs, coherently with considering the recent MN eruption as the first one of a new Epoch.

Figure 8 shows the cumulative volumes locally erupted by the main zones interested by the larger or recurrent explosive activity during Epochs I and III: it is remarkable to highlight the presence of clusters of events in time and space.

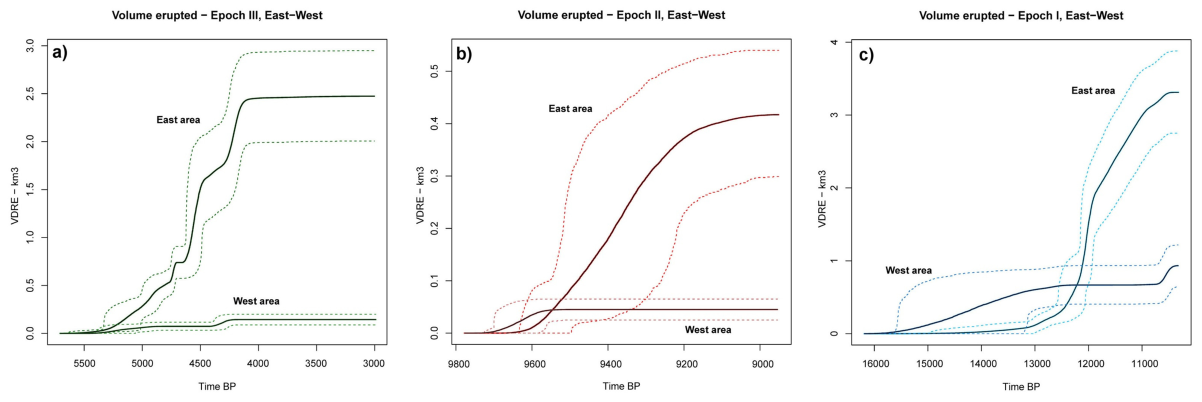

Fig 7. Cumulative volume erupted as a function of time during Epoch III (a), Epoch I (b) (c), separation between the East and the West of the caldera. The bold line is the mean value and the dashed lines are 5th and 95th percentiles of the uncertainty.

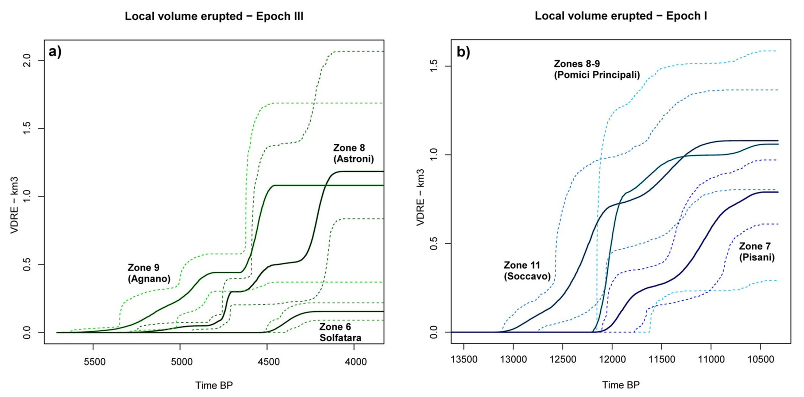

Fig 8. Localized cumulative volume erupted as a function of time during Epoch III (a) and Epoch I (b), from three different zones characterized by intense or recurrent activity. The bold line is the mean value and the dashed lines are 5th and 95th percentiles of the uncertainty.

A doubly stochastic point process modelling the vent clustering

Here it is defined a family of counting processes representing the number eruptive events that occurred in each zone of the caldera as a function of time. The family is taken in the class of Hawkes processes (see Daley and Vere Jones [2005, 2008]), able to reproduce the time clustering phenomena of explosive eruptions; we assume them doubly stochastic in the sense that the parameters are randomly distributed as a function of the sources of uncertainty considered.

A Hawkes process basically is a Poisson process whose intensity function λ depends on the previously observed events. In particular for each zone *j* of the caldera, the local intensity function is:

$$\lambda^j(t) = \lambda_0^j + \sum_i h e^{-k(t-t_i^j)},$$

where λ_0 is the local base rate (i.e. in absence of self-excitement), the array $(t_i^j)_i$ contains the times of eruptions occurred in the zone before time *t*; *k* and *h* are parameters tuning an exponential decay for the self-excitement.

A global base rate λ_0 is assumed for the whole caldera, and the local base rate of each zone is calculated in proportion to the frequency of the number of events observed in that location on the total. Also the parameters *k* and *h* are defined independently of the zone.

The parameter *k* is proportional to the time $T=k/ln(20)$ needed for the decay of the 95% of self-excitement (i.e. the integrated additional intensity on the times above *T* is 5% of the total). Moreover *h* permits to define the mean offspring $\mu=h/k$ of an eruption, i.e. the mean number of eruptions generated by the additional intensity caused by a single event. Some samples of the model are shown in Figure 9.

The likelihood of a time and space record of past eruptions can be easily expressed: hence the maximizing parameters have been calculated with uncertainty through a Monte Carlo simulation. In Table 2 are shown the corrrespondent uncertainty distributions of λ_0, *T*, *μ* for each epoch, and also the result of maximizing independently the likelihood of all three epoch's records.

EPOCH III	5th %ile	mean	95th %ile
base rate (λ0)	1/143	**1/103**	1/78
self excitement duration (T)	11	**90**	198
mean offspring (μ)	0.31	**0.42**	0.50
cluster generation probab.	27%	**34%**	39%
number of clusters	2.4	**4.0**	5.4
mean cluster size	2.7	**3.1**	3.6
cluster sizes			
(1)	73.5%	**65.7%**	60.5%
2	16.4%	**18.1%**	18.4%
3	5.8%	**7.4%**	8.4%
4	2.3%	**3.7%**	4.5%
5	1.1%	**2.1%**	2.7%
6	0.5%	**1.1%**	1.7%
7	0.2%	**0.6%**	1.2%
8	0.1%	**0.4%**	0.8%
9	0.1%	**0.3%**	0.4%
10	0.0%	**0.2%**	0.4%
offspring prob. after 476 yrs	0.0%	**0.0%**	0.0%
no erupt. for 476 yrs after MN	0.1%	**0.8%**	2.5%

EPOCH II	5th %ile	mean	95th %ile
base rate (λ0)	1/98	**1/64**	1/41
self excitement duration (T)	7	**103**	260
mean offspring (μ)	0.12	**0.24**	0.38
cluster generation probab.	11%	**21%**	32%
number of clusters	0.1	**0.4**	1.0
mean cluster size	2.2	**2.5**	2.9
cluster sizes			
(1)	88.6%	**78.8%**	68.7%
2	9.5%	**14.7%**	17.6%
3	1.5%	**4.3%**	6.9%
4	0.3%	**1.4%**	3.1%
5	0.0%	**0.5%**	1.6%
6	0.0%	**0.2%**	0.9%
7	0.0%	**0.1%**	0.5%
8	0.0%	**0.0%**	0.3%
9	0.0%	**0.0%**	0.2%
10	0.0%	**0.0%**	0.1%
offspring prob. after 476 yrs	0.0%	**0.0%**	0.1%
no erupt. for 476 yrs after MN	0.0%	**0.1%**	0.7%

EPOCH I	5th %ile	mean	95th %ile
base rate (λ0)	1/261	**1/159**	1/102
self excitement duration (T)	85	**525**	980
mean offspring (μ)	0.18	**0.34**	0.46
cluster generation probab.	16%	**29%**	37%
number of clusters	1.0	**3.2**	5.6
mean cluster size	2.4	**2.8**	3.3
cluster sizes			
(1)	83.5%	**71.3%**	63.1%
2	12.6%	**17.2%**	18.3%
3	2.8%	**6.3%**	8.0%
4	0.8%	**2.7%**	4.1%
5	0.2%	**1.2%**	2.3%
6	0.1%	**0.6%**	1.4%
7	0.0%	**0.3%**	0.9%
8	0.0%	**0.2%**	0.6%
9	0.0%	**0.1%**	0.4%
10	0.0%	**0.0%**	0.3%
offspring prob. after 476 yrs	0.0%	**2.8%**	7.8%
no erupt. for 476 yrs after MN	0.6%	**4.3%**	11.9%

ALL EVENTS	5th %ile	mean	95th %ile
base rate (λ0)	1/120	**1/97**	1/78
self excitement duration (T)	40	**124**	242
mean offspring (μ)	0.26	**0.37**	0.49
cluster generation probab.	23%	**31%**	39%
number of clusters	1.7	**3.2**	5.3
mean cluster size	2.5	**2.9**	3.5
cluster sizes			
(1)	77.2%	**68.9%**	61.3%
2	15.3%	**17.7%**	18.4%
3	4.7%	**6.8%**	8.3%
4	1.6%	**3.0%**	4.3%
5	0.6%	**1.6%**	2.6%
6	0.3%	**0.8%**	1.6%
7	0.1%	**0.5%**	1.1%
8	0.1%	**0.2%**	0.7%
9	0.0%	**0.1%**	0.5%
10	0.0%	**0.1%**	0.3%
offspring prob. after 476 yrs	0.0%	**0.0%**	0.1%
no erupt. for 476 yrs after MN	0.2%	**0.6%**	1.3%

Table 2. The parameters λ_0, *T*, *μ* maximizing likelihood of each dataset; the correspondent probability, number and mean size of the clusters of vents; the distribution of their size; the probability of having an offspring after 476 yrs, and of passing 476 yrs without eruptions after an event. Mean values, 5th and 95th percentiles are shown, as a function of the sources of uncertainty considered.

Other interesting information is obtained from the model: the probability *P* of an eruption to generate offspring, the mean number and size of clusters of two or more events, and the probability distribution on the possible cluster sizes. Assuming such simple model, the residual probability of having an offspring of MN in the future and the probability of not observing any eruption for 476 yrs after the first have been also calculated: both are significantly small.

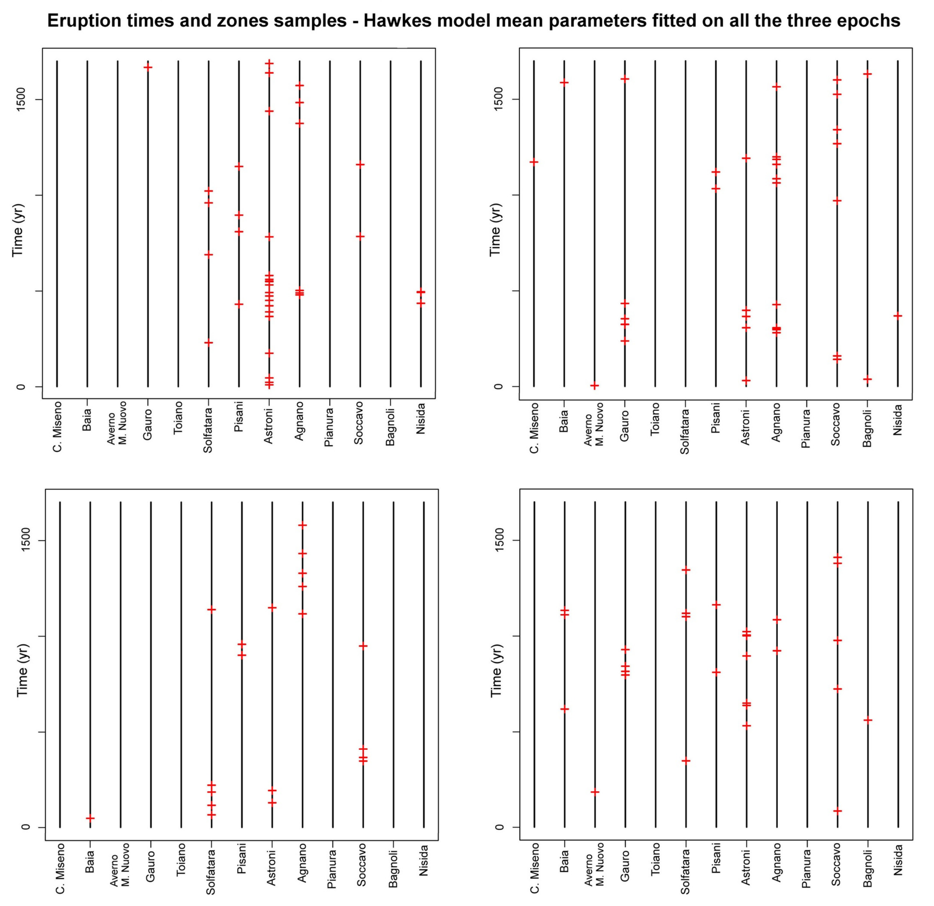

Fig 9. Four random samples of eruption times and zones obtained from the Hawkes model described above. The parameters adopted are the average values of maximum likelihood for the entire record of the three epochs: λ_0= 1/97 yrs⁻¹, *T*=124 yrs, *μ*=0.37. Each coloured line represents an event.

Concluding remarks

Analysis of the new model confirms earlier appreciations of spatio-temporal clustering in the Campi Flegrei, but the quantified self-excitement duration appears to be shorter than the time passed after MN in AD 1538, except for the data of the Epoch I. For this reason the location of MN eruption seems not to be more informative than the places of the previous eruptions for what concerns the next eruptive event forecasting, moreover the maximum likelihood probability of not developing a cluster remains in general above 60% for every of the records available.

Anyways the 476 yrs intercurred between MN and the present time without observing any other events are still difficult to explain with the simple model presented and assuming MN as the first eruption of Epoch IV, except for looking at the very uncertain dataset of Epoch I alone. A research focused on the first part of each epoch and in particular on the transitions from the periods of quiescence to the eruptive activity is of the main importance.

In addition to this, the volumes erupted from the East of the caldera are remarkably greater than the volumes from the West, although both are affected by a large uncertainty furthermore very difficult to quantify precisely. Such a correlation between the spatial location and the size of the explosive eruptions could be motivated considering the different geologic structures involved, and it is crucial to understand the consequences of treating separately the East and the West of Campi Flegrei, also in terms of hazard estimation.

Acknowledgement: has been partially developed during the projects DPC-V1 and MED-SUV, funded by Dipartimento della Protezione Civile (Italy) and the European Commission.

References:

Bebbington, M.S. and S.J. Cronin (2011), Spatio-temporal hazard estimation in the Auckland Volcanic Field, New Zealand, with a new vent-order model, Bull. Volcanol., 73, 55-72.

Bevilacqua, A., R. Isaia, A. Neri, S. Vitale, W. P.Aspinall, M. Bisson, F. Flandoli, P. J. Baxter, A. Bertagnini,T. Esposti Ongaro, E. Iannuzzi, M. Pistolesi, M. Rosi (2014), Quantifying volcanic hazard at Campi Flegrei caldera (Italy) with uncertainty assessment: I. Vent opening maps, JGR-solid Earth (submitted)

Daley, D.J., D. Vere Jones (2005, 2008), An Introduction to the Theory of Point Processes, Volume I – II, Springer.

Klawonn, M., B.F. Houghton, D.A. Swanson, S.A. Fagents, P. Wessel, C.J. Wolfe (2014), From field data to volumes: constraining uncertainties in pyroclastic eruption parameters, Bull. Volcanol. 76.

Smith, V.C., R. Isaia and N.J.G. Pearce (2011),Tephrostratigraphy and glass compositions of post-15 kyr Campi Flegrei eruptions: Implications for eruption history and chronostratigraphic markers, Quatern. Sci. Rev., 30, 3638-3660.